

# Static and Dynamic Measurements Using Embedded Earth Pressure Cells

GEORGE M. FILZ AND THOMAS L. BRANDON

As part of a research program to study lateral earth pressures on retaining walls, dynamic compactor forces were measured by two methods: (a) a direct instrumentation method that is thought to yield reliable measurements of dynamic compactor forces and (b) taking measurements of embedded earth pressure cell responses that are converted to estimated compactor forces at the ground surface. Comparison of the compactor forces from the two methods disclosed the following. (a) Reflection of seismic waves from the boundaries of the backfill can create a standing wave at the embedded pressure cell location, which may cause pressure cells to overregister. (b) The pressure distribution beneath the base of the compactor can influence the embedded pressure cell readings. (c) Use of a registration ratio of unity resulted in estimated compactor forces that were generally in as good, or better, agreement with the forces measured by the direct instrumentation as when in situ registration ratios were used. During the in situ calibration studies, several factors that can influence the response of embedded pressure cells to static loads were identified: the presence of clods in the backfill can influence pressure cell response, even when the diaphragm size to soil particle size criterion is well satisfied; compaction-induced lateral earth pressures can cause nonlinearity in pressure cell response because of the rotation of lateral stresses; and other factors, such as variations in cell placement conditions, can influence pressure cell results.

A research program to study the effects of backfill compaction on the lateral earth pressures that act on retaining walls is under way at Virginia Polytechnic Institute and State University. Because dynamic compactor forces have an important influence on the magnitude of compaction-induced lateral pressures, the research work included compactor force measurements.

Embedded earth pressure cell measurements have been used by others (1-3) to estimate the magnitudes of dynamic compactor forces. In the present study, both earth pressure cells and instrumentation installed directly on the compactor were used to measure compactor forces. Comparison of the embedded pressure cell readings with forces measured by "direct" methods provided insight into the significance of factors that influence pressure cell readings under dynamic compactor loading.

The purpose of this paper is to describe the sources of uncertainty in using embedded pressure cell readings for determining dynamic compactor forces. Some of these factors can also be important for static pressure cell measurements.

## INSTRUMENTAL RETAINING WALL TESTS

### Instrumented Retaining Wall Facility

A cross section through the instrumented retaining wall facility is shown in Figure 1. The backfill area is 1.8 m wide and 3.0 m

long. Backfill is typically placed about 2.0 m high against the wall, which is 3.0 m long and 2.1 m high. The wall consists of four panels located within a very stiff reinforced concrete structure. Each panel is 0.8 m long and 2.1 m high. The panels are supported by load cells so that the horizontal and vertical forces applied by the backfill can be measured. The center two panels are instrumented with 15 contact pressure cells so that the pressure distribution on the wall can be determined. The instrumented retaining wall facility is described in detail by Sehn and Duncan (4), and the performance of the contact pressure cells in the instrumented wall is described by Filz and Duncan (5,6).

A total of 16 tests have been performed in the instrumented retaining wall facility at Virginia Polytechnic Institute and State University. Of these, embedded earth pressure cells were used in six tests and direct measurements of dynamic compactor forces were made in five tests. These tests and some key test parameters are given in Table 1.

### Backfill Soils

Two soil types were used in the present study: Yatesville silty sand and Light Castle sand. Yatesville silty sand is an alluvial soil excavated from the foundation of Yatesville Lake Dam on Blaine Creek in Lawrence County, Kentucky. Yatesville silty sand classifies as an SM soil by the Unified Soil Classification System and contains about 47 percent nonplastic fines. The mean grain size ( $D_{50}$ ) of the soil is about 0.08 mm. The soil has a maximum dry density of 19.6 kN/m<sup>3</sup> and an optimum water content of 11 percent for the standard Proctor effort (standard ASTM D698-91). The specific gravity of solids is about 2.67. When in moist condition the Yatesville silty sand has an apparent cohesion from negative pore water pressure and will stand on vertical slopes several feet high.

Light Castle sand is a clean, fine, quartz sand obtained from a quarry in Craig County, Virginia. The sand classifies as an SP soil by the Unified Soil Classification System and has less than 1 percent fines. The  $D_{50}$  of the soil is 0.3 mm. The maximum and minimum densities according to standards ASTM D4253-83 and ASTM D4254-83 are 16.65 and 13.90 kN/m<sup>3</sup>, respectively. The specific gravity of soils is about 2.65. The Light Castle sand was placed and compacted in a dry condition and, when dry, was completely cohesionless.

### Compactors

Two types of hand-operated compaction equipment were used in the study: a rammer compactor and a vibrating-plate compactor. The compactor usage is given in Table 1.

Charles E. Via, Jr., Department of Civil Engineering, Virginia Polytechnic Institute and State University, Blacksburg, Va. 24061-0105.

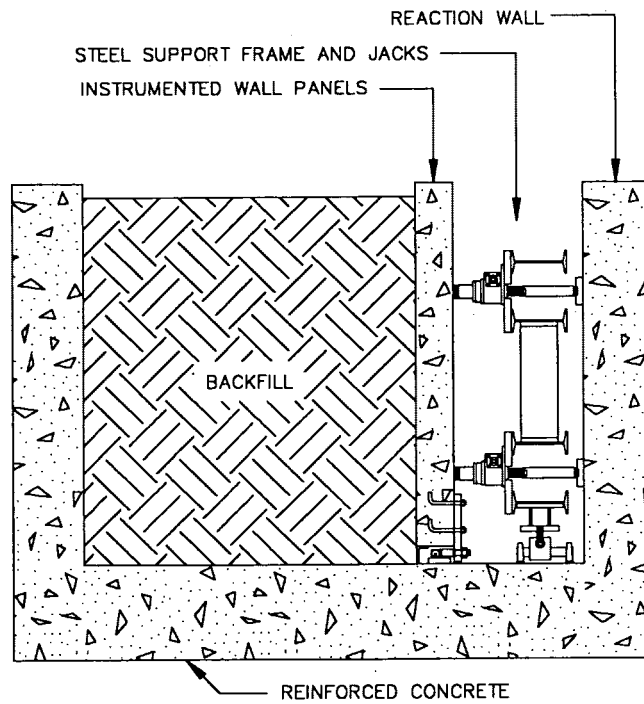


**FIGURE 1** Cross section through the instrumented retaining wall facility.

The rammer compactor is a hand-operated Wacker model BS60Y. It is powered by a 3000-W (4 hp), two-cycle engine that drives a ramming shoe into contact with the soil at a percussion rate of about 10 blows per sec. The operating weight of the compactor is 62 kg (137 lb). The vibrating-plate compactor is the hand-operated Wacker model BPU2440A. It is powered by a 3700-W (5 hp), four-cycle engine that drives counterrotating eccentric weights. The eccentric weights rotate at a frequency of about 100 Hz on axles fixed to a steel base plate that contacts the soil. The operating weight of the compactor is 125 kg.

As mentioned previously, instrumentation was attached directly to both compactors to measure the dynamic compactor forces imparted to the backfills. Details of this instrumentation, the instrumentation verification studies, and the resulting force measurements obtained during the instrumented retaining wall tests are presented by Filz and Brandon (7). The following paragraphs summarize the instrumentation schemes.

For the rammer compactor, dynamic load cells were installed between the rammer shoe and the main body of the compactor, and accelerometers were mounted on the rammer shoe. The con-

**TABLE 1** Instrumented Retaining Wall Tests with Embedded Pressure Cell Measurements and Dynamic Compactor Force Measurements

Test No.	Soil Type <sup>(1)</sup>	Water Content (%)	Dry Unit Weight kN/m <sup>3</sup>	Compactor Type <sup>(2)</sup>	Peak Dynamic Compactor Force <sup>(3)</sup> (kN)		
					Average	Std. Dev.	No. of Readings
EP 10	YSS	11.8	17.25	Vib	N/A	N/A	N/A
EP 12	YSS	12.3	17.32	Vib	5.4	0.7	12
EP 13	YSS	12.7	18.77	Ram	22.4	2.1	10
EP 14	YSS	10.1	18.63	Ram	32.6	4.3	9
EP 15	LCS	0.0	16.68	Ram	21.3	5.0	15
EP 16	LCS	0.0	16.45	Vib	5.8	1.2	16

Notes: (1) YSS indicates Yatesville silty sand. LCS indicates Light Castle Sand.

(2) Vib indicates the Wacker BPU2240A vibrating plate compactor. Ram indicates the Wacker BS60Y rammer compactor.

(3) The direct measurements were obtained from instrumentation attached directly to the compactors.

tact force between the bottom of the rammer shoe and the soil was determined by measuring the force on top of the shoe and adding the mass times acceleration of the shoe.

For the vibrating-plate compactor, load cells could not conveniently be installed to measure the force on the top of the compactor base plate. Instead, the force was calculated by summing the masses times the accelerations of the three principal compactor components: the upper mass, the eccentric weights, and the base plate. One accelerometer was mounted on the upper mass so that its mass times acceleration could be determined. For the eccentric weights, a Hall effect device (HED) was used to measure the shaft rotation rate and to start the data acquisition at a known shaft position so that the force component from the eccentric weights could be added to the other force components. Another accelerometer was mounted on the compactor base plate so that its mass times acceleration could be determined. The sum of these three force components is equal to the contact force between the base plate and the soil.

A statistical summary of the dynamic compactor force measurements is given in Table 1. For a given compactor, the force magnitude depends primarily on the stiffness of the compacted soil. The rammer compactor provided an average dynamic force of about 24.5 kN. The vibrating-plate compactor provided an average dynamic force of about 5.7 kN.

## EMBEDDED PRESSURE CELLS

### Description of Kulite Cells

The pressure cells used in the present study were Kulite soil pressure cells, Type 0234, manufactured by Kulite Sensors, Ltd. A schematic drawing of a cell is shown in Figure 2. The cells contain a semiconducting silicone diaphragm at the base of a fluid-filled chamber. Pressure is applied to the silicone diaphragm through the fluid via a stainless steel reinforcing plate and isolation diaphragm. The reinforcing plate is separated from the main body of the sensor by a silicone annulus.

### Factors That Influence Cell Performance

In their comprehensive summary, Weller and Kulhawy (8) use the concept of the registration ratio,  $R$ , to describe the factors

that influence the performance of embedded earth pressure cells:

$$R = \frac{\sigma_c}{\sigma_s}$$

where  $\sigma_c$  is the normal stress measured by a cell on the basis of its fluid calibration and  $\sigma_s$  is the free-field normal stress present in the soil. When  $R$  is greater than 1.0, a cell is said to *overregister*. When  $R$  is less than 1.0, a cell is said to *underregister*. The principal influential factors identified by Weller and Kulhawy (8) are given in Table 2, together with recommended correction or control methods.

The Kulite cells meet the criteria suggested by Weller and Kulhawy (8) in most respects. However, the aspect ratio of the Kulite cells ( $T/D = 0.284$ ) does not satisfy the recommended aspect ratio criterion of  $T/D < 0.2$ . Because the Kulite cells generally satisfy the recommended criteria in so many respects, it was anticipated that they would perform well in the present application.

### Previous Use of Kulite Pressure Cells

Kohl et al. (9) describe an application in which Kulite cells were used to measure static and dynamic stresses in the vicinity of buried pipelines. Their findings included the following:

- During in-soil laboratory calibrations, registration ratios ranged from 1.03 to 1.45 for the first cycle of loading.
- During in-soil laboratory calibrations, registration ratios decreased with increasing stress magnitude.
- During in-soil laboratory calibrations, substantial hysteresis was observed in ( $K_0$ ) loading-unloading cycles.
- During field tests, the initial measured stresses were greater than the calculated overburden stress.
- During field tests, the ratio of the peak dynamic load from a moving truck wheel to the static wheel load from the parked truck varied between 0.9 and 1.8. For a truck traveling at 5 m/sec, the load pulse duration was a little less than 0.2 sec.

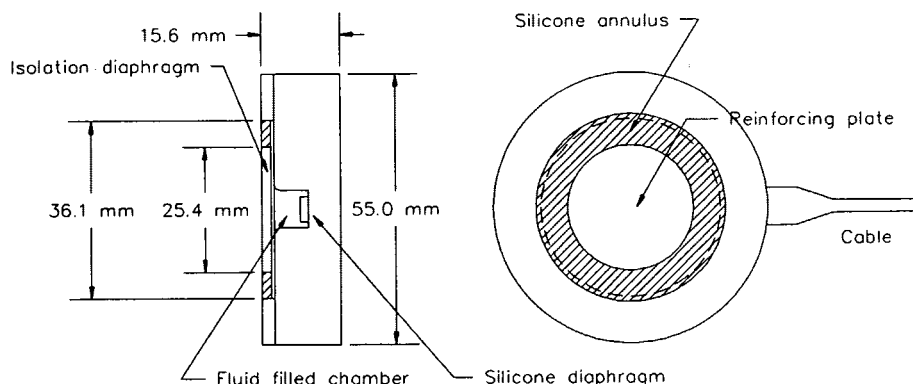


FIGURE 2 Kulite earth pressure cells.

TABLE 2 Factors Influencing Stress Cell Measurements (8)

Factor	Effect	Recommended Correction/Control Method
Aspect Ratio (cell thickness to diameter ratio)	Cell thickness alters stress field around cell.	$T/D < 0.2$
Soil-Cell stiffness ratio, S	At low values of S, small changes in soil stiffness do not cause significant changes in cell registration. At high values of S, changes in soil stiffness cause nonlinear registration.	$S < 0.5$
Diaphragm deflection (arching)	Excessive deflection can cause underregistration due to soil arching over the diaphragm.	$d/D > 2000-5000$
Stress concentrations at cell corners	Can cause a stiff cell to overregister unless the active area is small compared to the overall cell area.	$d^2/D^2 < 0.25-0.45$
Point loads	If the active area is not sufficiently large compared to the soil particle size, non-uniform load distribution can cause registration errors.	$d/D_{50} > 10$ to 50
Lateral stress rotation	The presence of a stiff cell in the soil causes a portion of the lateral stresses to be registered as normal stresses.	Use correction factors.
Cross-sensitivity	Lateral compression of a cell register as a normal stress.	Change strain gauge arrangement or add outer rings.
Stress-strain behavior of soil during calibration	Cell readings are influenced by the soil stress-strain response and the calibration conditions, i.e., $K_0$ or triaxial conditions.	Calibrate cells under field conditions.
Placement effects	Non-uniform conditions in the vicinity of the cell can cause erroneous response.	Use consistent, reproducible placement procedures for calibration and field installations.
Proximity of structures and other stress cells	Interaction of stress fields can cause measurement errors.	Use adequate spacing.
Dynamic stress measurements	Cell response time, differences between cell and soil density, and differences between cell and soil impedance can cause errors.	Use resistance or semiconductor strain gages, stiff cells, and dynamic calibration.

Note:  $D_{50}$  = mean grain size of soil

## STATIC OVERBURDEN PRESSURE MEASUREMENTS IN INSTRUMENTED RETAINING WALL TESTS

### Influence of Placement Condition

As indicated in Table 1, instrumented retaining wall test EP 10 was the first test in which embedded Kulite pressure cells were installed. In that test, the vibrating plate was used to compact the moist Yatesville silty sand backfill soil. The walls of the facility were lubricated with alternating layers of grease and plastic to reduce shear stresses between the compacted soil and the walls. Measurements on the instrumented wall indicated that this treatment effectively reduced the friction coefficient to about 0.02 (5), so that the vertical stress, for practical purposes, was equal to the depth times the unit weight of the backfill. This condition permitted in situ calibrations of the embedded pressure cells to be obtained.

The backfill placement procedures were similar for all the tests with embedded pressure cells. The backfill was placed in hand-raked, loose lifts of sufficient thickness to produce compacted lifts 150 mm thick. The Kulite cells were placed after three lifts of backfill had been compacted. Thus, they were located about 450 mm above the facility floor. After cell placement, backfill place-

ment and compaction continued in lifts until a total of 2.0 m of backfill had been placed, resulting in 1.5 m of backfill over the cells.

Three different cell placement conditions were used in test EP 10: recessed, flush, and projecting. These conditions, as well as the in situ calibrations, are shown in Figure 3(a). According to the best-fit lines in Figure 3(a), the recessed placement condition yielded the lowest registration ratio (0.69), the flush placement condition yielded a higher registration ratio (0.82), and the projecting placement condition yielded the highest registration ratio (1.25). The trend of higher registration with greater cell projection was expected.

Figure 3(b) shows the secant registration ratios plotted versus overburden stress. The reason for the very low registration ratios at low overburden pressures is not known.

Since flush placement yielded the registration ratio closest to unity, the flush condition was used for the remaining instrumentation retaining wall tests that were backfilled with moist Yatesville silty sand. This is consistent with the method used by Hadala (10) for clay soil. For the cohesionless Light Castle sand, the cells were placed on the top of the previously compacted lift, and subsequent backfilling progressed as if the cells were not present. This is consistent with the method used by Hadala (10) for sand.

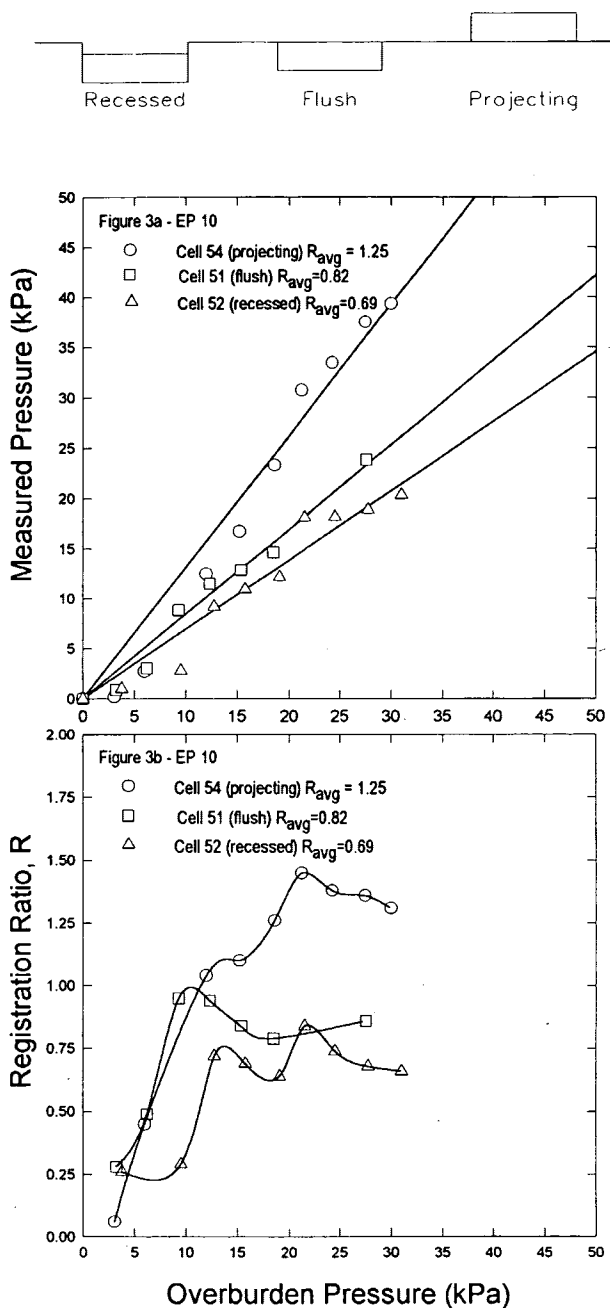


FIGURE 3 Measured pressures and registration ratios for test EP 10.

#### Influences of Soil Type, Soil Water Content, and Compaction Plant

The in situ calibrations for instrumented retaining wall tests EP 12 through EP 14 are shown in Figure 4 and those for tests EP 15 and EP 16 are shown in Figure 5. Cell placement conditions, the presence of clods in the backfill, compaction-induced lateral pressures, and soil modulus may have all influenced pressure cell registration. These factors are discussed in the following paragraphs.

The backfill for test EP 12 was moist Yatesville silty sand that was compacted with the vibrating-plate compactor. Figure 4(a)

shows that the response was approximately linear for each cell but that the registration ratio varied among the three cells installed. The registration ratio for cell 53 was consistently about 35 percent higher than the average registration ratio for all three cells. This occurred even though care was taken to install all three cells using the same flush placement condition. This could have occurred because of small, undetected differences in cell placement conditions. However, it is also possible that clods within the Yatesville silty sand backfill protected the diaphragms of cells 50 and 54 from the full overburden load. The vibrating-plate compactor did not impose a large contact force and was not well able to break down clods into a uniform backfill material. Thus, even though the active diaphragm size criterion is easily satisfied ( $d/D_{50} = 450 \gg 10$  to 50), the presence of clods in the backfill can control the transfer of stress to small diaphragms, Dunicliff (11) makes the general recommendation that embedded pressure cells be 230 to 300 mm in diameter. Cells of that size, which greatly exceeds the Kulite cell size, would have been less influenced by clods in the backfill.

The backfill for test EP 13 was wet Yatesville silty sand that was compacted with the rammer compactor. Figures 4(c) and (d) show that the response is approximately linear for each cell and that the registration ratio is close to unity for all three cells. The rammer compactor applied a large force to the backfill and was able to break down clods in the wet Yatesville silty sand to form a uniform material.

The backfill for test EP 14 was dry Yatesville silty sand that was compacted with the rammer compactor. Figures 4(e) and (f) show a nonlinear cell response, with decreasing registration ratios as the applied pressure increases. Over the applied stress range, the registration ratios generally exceeded unity. Two aspects of the data in Figures 4 (e) and (f) are especially interesting.

1. The nonlinear response: The nonlinearity could be caused by lateral stress rotation or by changes in the soil stiffness. The lateral earth pressures measured at the instrumented wall are shown in Figure 6. The pressure distributions are approximately linear for tests EP 12 and EP 13, and lateral stress rotation would not be expected to induce nonlinearity in the registration ratios for these tests. The lateral pressure distribution for test EP 14, on the other hand, is strongly nonlinear, with significant compaction-induced lateral earth pressures evident in the upper portion of the plot. Rotation of the compaction-induced lateral earth pressures owing to the presence of the rigid pressure cells would be expected to cause nonlinearity in pressure cell registration. It is also possible that increases in the soil stiffness as the stress level is increased could cause a decrease in the registration ratio. However, as shown in Table 2, if the soil-cell stiffness ratio is low, the cell response should not be very sensitive to changes in soil stiffness. For this reason, lateral stress rotation is probably the larger contributor to the nonlinear registration shown in Figures 4(e) and (f). The type of nonlinearity shown in Figure 4(e) is similar to that reported by Kohn et al. (9) for  $K_0$  unloading in laboratory calibration tests. The cause of the curvature is probably the same in both cases: rotation of high lateral stresses at low vertical stresses.

2. The difference between the responses of the two cells: The registration ratios for the two cells used in test EP 14 differed from their average value at any applied stress level by about 20 percent. Like test EP 13, the Yatesville silty sand backfill used in EP 14 was compacted with the rammer compactor; however, the backfill was relatively dry, so that the clods were more difficult

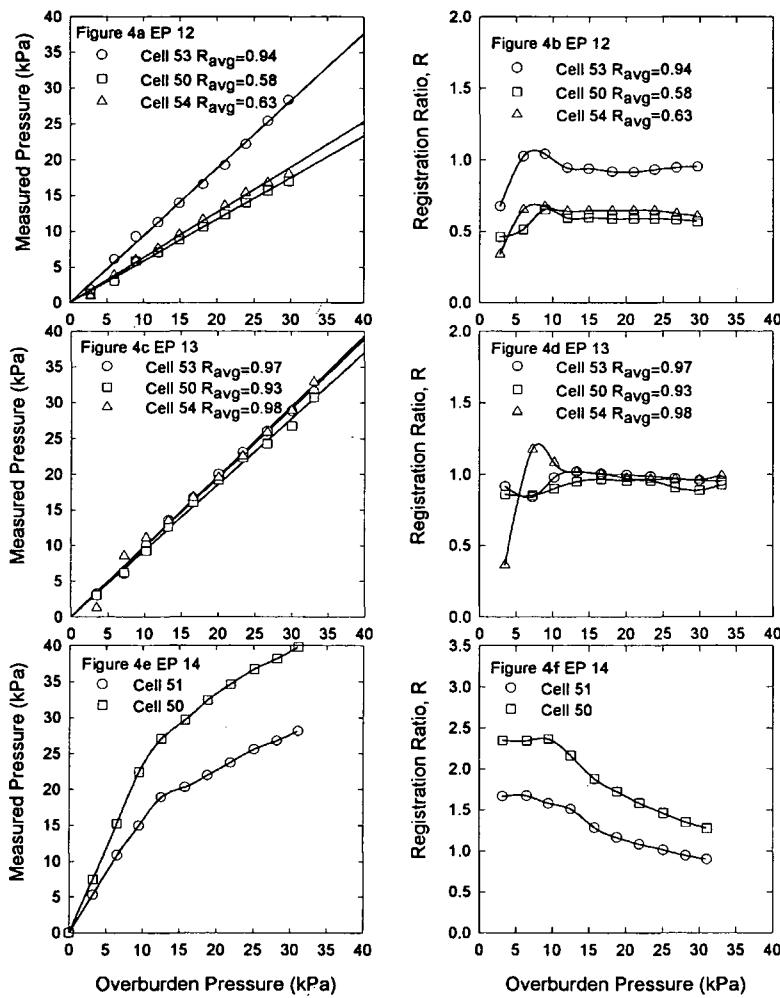


FIGURE 4 Measured pressures and registration ratios for tests conducted in Yatesville silty sand.

to break down for test EP 14 than for test EP 13. Thus, the presence of clods could have contributed to the difference in registration for the two cells used in test EP 14.

The backfill for test EP 15 was dry Light Castle sand that was compacted with the rammer compactor. Figures 5(a) and (b) show nonlinear cell responses, with increasing and then decreasing registration ratios as the applied pressure increases. Over the applied stress range, the registration ratios generally exceeded unity. The reason for the observed variations in registration ratios is not known, particularly for the increasing registration ratios at low stresses. The decreasing registration ratios at higher stresses could have been due to compaction-induced lateral stress rotation or increases in soil stiffness, as described for test EP 14. It is also possible that the cell placement condition (i.e., nonuniform soil conditions in the immediate vicinity of the cell) could have changed during compaction of the overlying lifts. In addition to the observed nonlinearity, there was a significant difference between the registration ratios of the two cells, up to about 15 percent difference from their average value. The difference was smaller than that for tests EP 12 and EP 14, but it was still significant. For the Light Castle sand, the active diaphragm size criterion was also easily satisfied ( $d/D_{50} = 120 \gg 10$  to 50), but, in

contrast to tests EP 12 and EP 14, no clods formed. Care was exercised to achieve the same placement condition for both cells. The difference in registration ratios is not easily explained. The most likely explanation is that, because of their small size, the Kulite cells are sensitive to relatively small differences in placement condition that are difficult to detect.

The backfill for test EP 16 was dry Light Castle sand that was compacted with the vibrating-plate compactor. Figures 5(c) and (d) show nonlinear cell responses, with increasing and then decreasing registration ratios as the applied pressure increases. The response was similar to that for test EP 15, and the same comments apply.

#### DYNAMIC PRESSURE MEASUREMENTS DURING COMPACTOR OPERATION

In addition to the sources of error and uncertainty to which static earth pressure measurements are subject, dynamic measurements during compactor operation can be influenced by differences between the density and impedance of the soil and the cell, rate-dependent variations in the soil stress strain properties, and differences between the cell placement condition during dynamic

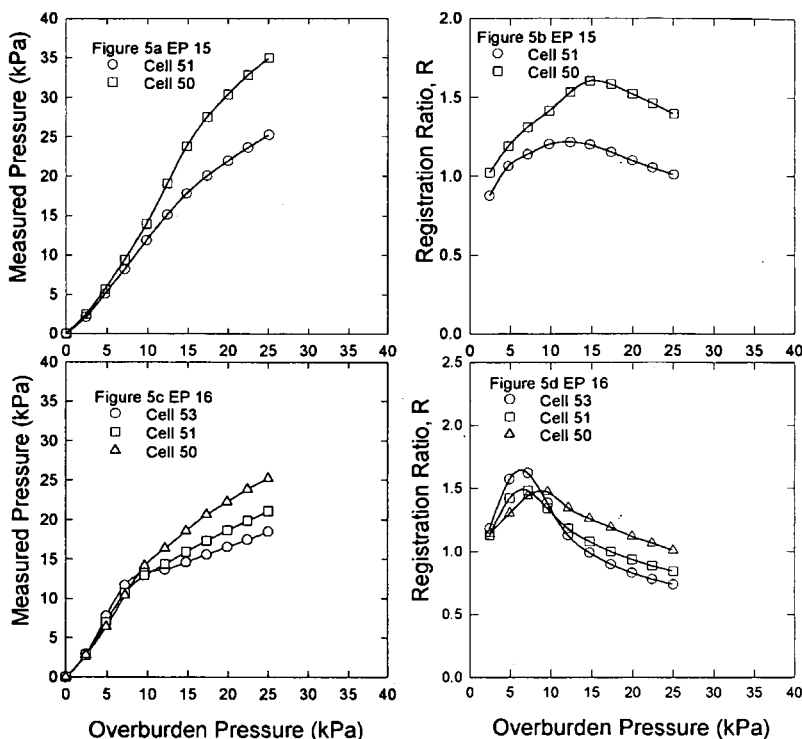


FIGURE 5 Measured pressures and registration ratios for tests conducted in Light Castle sand.

loading and subsequent static loading from overlying fill lifts. In addition, since the compactor loads a finite area on the lift surface a short distance above the cell, the problems of stress distribution with depth and nonuniform pressure distribution at the contact must be considered. Also, the position of the cell relative to the compactor base plate may not be exactly known at the time of the measurements. All of these factors may have influenced the

accuracy of the pressure cell readings as a means for determining dynamic compactor forces. The following paragraphs describe the dynamic measurements and discuss the influences that these factors may have had on the results.

**Data Acquisition and Data Reduction Procedures**

In all cases, measurements were taken during compactor operation on the next lift after cell placement so that the cells were at a depth of about 150 mm below the compactor base plate. The instrumentation on the compactor and the embedded pressure cell were monitored with a high-speed data acquisition system.

Because the pressure cells were located one lift below the compactor base plate and because the cells measured pressure over a small area in comparison with the compactor base plate area, an analytic procedure is necessary to convert the pressure cell readings to a compactor contact force at the surface. The compactor base plates are relatively rigid, and the pressure distributions are not expected to be uniform. In fact, the pressure distributions depend on the characteristics of the soil being compacted, as shown in Figure 7. For a cohesionless soil, the pressure may be greatest beneath the center of the loaded area. For a cohesive soil, the pressure may be lowest beneath the center of the loaded area. Since the shapes of the pressure distributions were not known and to adopt a consistent procedure for all of the tests, the Boussinesq theory was used to obtain the uniform pressure distribution at the surface that would have caused the observed pressure cell reading. The compactor force from the pressure cell readings was then calculated by multiplying the computed uniform pressure at the surface by the compactor base plate contact area; these values

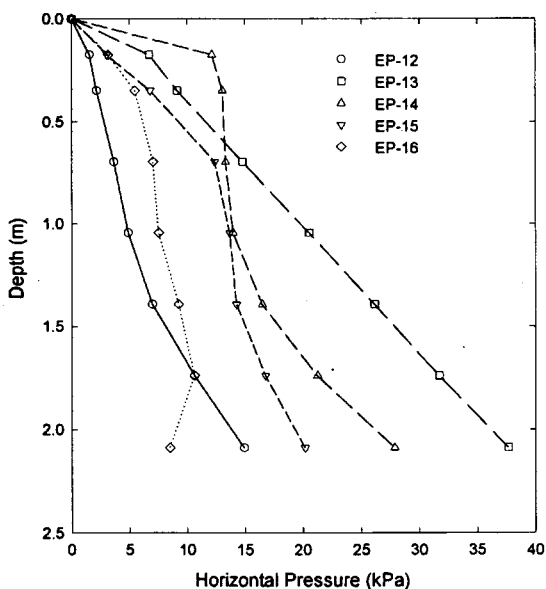
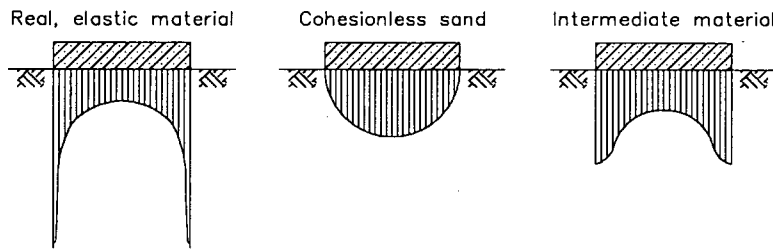


FIGURE 6 Horizontal earth pressures measured for tests EP 12 through EP 16.



**FIGURE 7** Contact pressures acting on the base of a smooth, rigid footing on different materials [after Terzaghi and Peck (12)].

were 1450 cm<sup>2</sup> for the vibrating-plate compactor and 550 cm<sup>2</sup> for the rammer compactor.

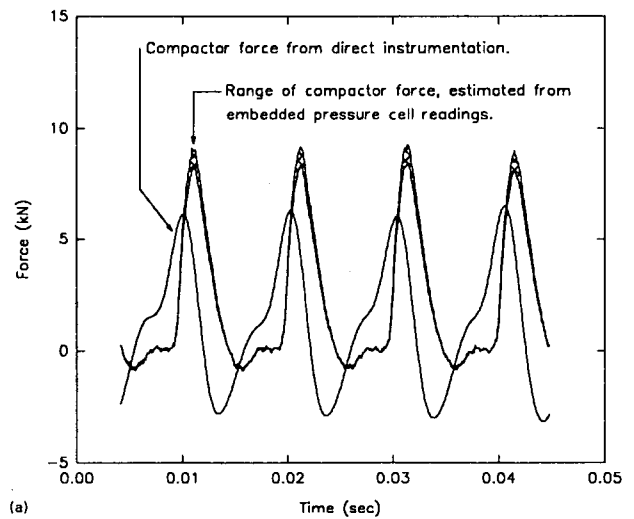
Even though an effort was made to operate the compactors directly over the pressure cells as the measurements were being taken, there was some uncertainty in the relative locations of the compactors and pressure cells. To account for this uncertainty, the Boussinesq calculations were performed by considering the possibility that the pressure cell could have been away from the center of each compactor base plate by as much as 50 mm. This resulted in a range of estimated compactor forces for each pressure cell reading.

The foregoing procedure can be performed by using a registration ratio of unity or a registration ratio obtained from Figures 4 and 5. The influence of using different values of the registration ratio is discussed in the next section.

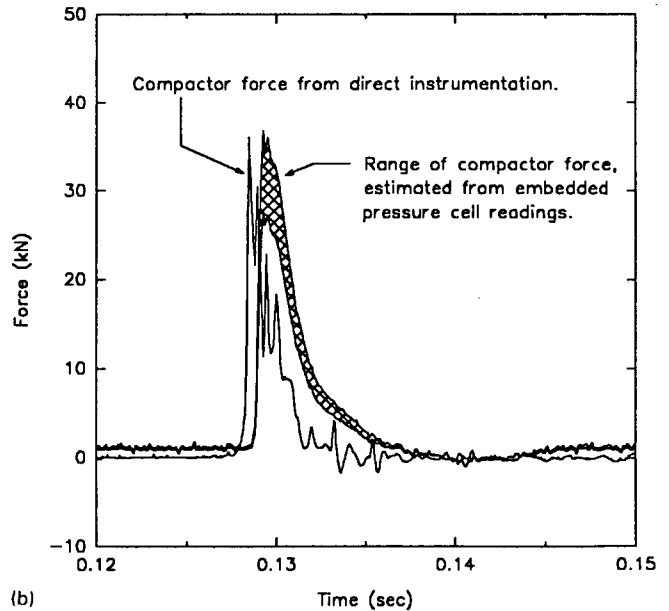
**Comparison of Estimated Compactor Force from Embedded Pressure Cell Measurements to Compactor Force from Direct Instrumentation**

Figure 8(a) shows a typical force versus time trace for the vibrating-plate compactor operating on the Yatesville silty sand. Both the compactor force from the direct instrumentation and the range of estimated compactor forces from the embedded pressure cell readings are shown. In Figure 8(a), a registration ratio of unity was used to obtain the force from the embedded pressure cell readings. The peak compressive force from the direct instrumentation is about 6.3 kN in this case. The peak compressive force estimated from the pressure cell measurements is about 8.0 kN. Use of the registration ratio for cell 54 in test EP 12 from Figure 4(a) would have resulted in even greater disparity between the force traces in Figure 8(a). One possible reason that the estimated force from the pressure cell exceeds the force from the direct instrumentation is that a standing wave could have developed at the pressure cell location from wave reflection off the floor of the instrumented retaining wall facility. Other reasons for the difference include the sources of error for dynamic applications of embedded earth pressure cells mentioned previously. Other interesting features of the data in Figure 8(a) include the following:

- The time lag between the force pulse at the surface and the force pulse at the pressure cell location: The time lag is about



(a)



(b)

**FIGURE 8** Vibratory compactor forces (a) and rammer compactor forces (b) measured from direct instrumentation and using embedded pressure cells.



0.001 sec, and the depth to the cell is about 150 mm. This corresponds to a compressive wave velocity of about 150 m/sec in the Yatesville silty sand backfill of test EP 12.

- The development of a tensile force during each compactor cycle: A small tensile stress, or "suction," between the smooth base plate of the vibratory compactor and the moist Yatesville silty sand during rapid unloading could account for the tensile force. The pressure cell readings appear truncated at about the zero pressure level.

Figure 8(b) shows a typical force versus time trace for the rammer compactor on the Yatesville silty sand. Again, a registration ratio of unity was used to obtain the force from the embedded pressure cell readings. In this case, the peak compressive forces from the direct instrumentation and the embedded pressure cell readings are similar, about 31.1 or 35.6 kN. The time lag is about 0.0007 sec, and the compressive wave velocity is about 210 m/sec.

Figure 9(a) shows a comparison between the estimated forces from the pressure cell readings and the forces from direct instrumentation for all the measurements made as part of the research described here. The comparison in Figure 9(a) is based on a registration ratio of unity. It can be seen that the data fall into three groups. For the rammer compactor operating on the Yatesville silty sand, the estimated forces from the pressure cells readings tend to be slightly less than the forces from the direct instrumentation. For the rammer compactor operating on the Light Castle sand, the estimated forces from the pressure cells readings are significantly greater than the forces from the direct instrumentation. The difference between these two groups could be accounted for by different pressure distributions on the rammer compactor base plate, as suggested by Figure 7. The high pressure expected under the base of the relatively rigid rammer base plate when operated on cohesionless Light Castle sand could explain the high estimated compactor forces from the pressure cell readings in this case.

For the vibrating-plate compactor, the data for both the Yatesville silty sand and the Light Castle sand seem to fall into the same group. The base plate of the vibrating-plate compactor is much larger than that of the rammer compactor, so contact stress distribution effects are not expected to be significant for the vibrating-plate compactor as they are for the rammer compactor. As mentioned previously, the occurrence of a standing wave at the pressure cell locations could have contributed to the apparent overregistration of the embedded pressure cells in this case.

Figure 9(b) shows a comparison between the estimated forces from the pressure cell readings and the forces from direct instrumentation when the registration ratios from Figures 4 and 5 are used to reduce the data. It can be seen that the correspondence between the forces determined by the two methods is slightly improved for the rammer compactor on the Light Castle sand, not significantly changed for the rammer compactor on the Yatesville silty sand, and made worse for the vibrating-plate compactor on both soil types. This result suggests that not much is to be gained by using registration ratios different from unity for obtaining dynamic forces from embedded pressure cell readings.

## SUMMARY AND CONCLUSIONS

As part of a research program to study lateral earth pressures on retaining walls, dynamic compactor forces were measured by two

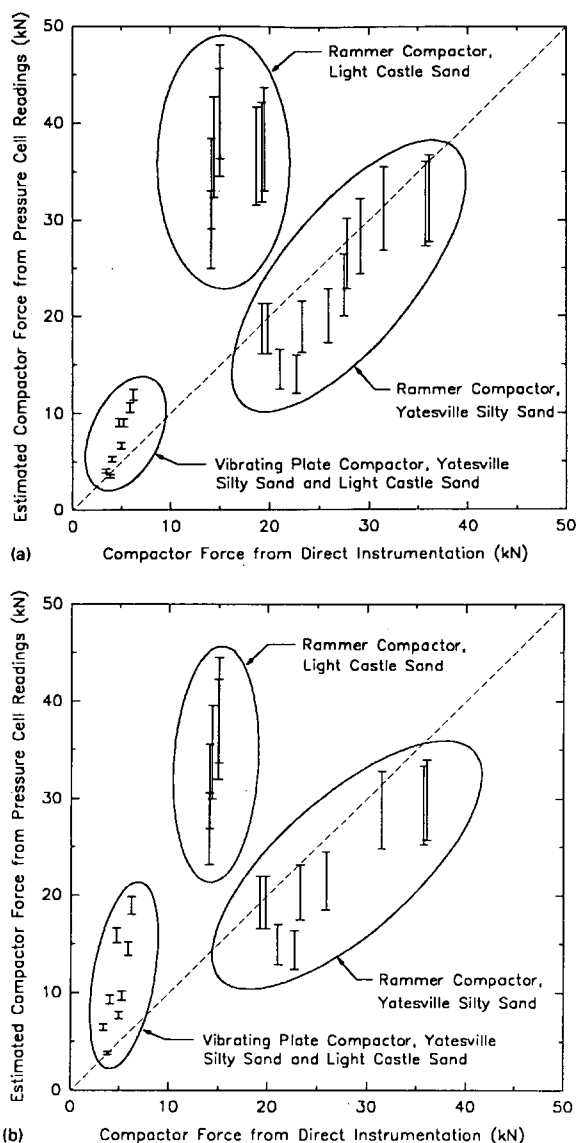


FIGURE 9 Comparison of compactor forces using a registration ratio of 1 (a) and in situ calibration factors (b).

methods: (a) a direct instrumentation method that is thought to yield reliable measurements of dynamic compactor forces and (b) taking measurements of embedded earth pressure cell responses that are converted to estimated compactor forces at the ground surface. Comparison of the compactor forces obtained by the two methods disclosed the following:

- Reflection of seismic waves from the boundaries of the backfill can create a standing wave at the embedded pressure cell location. In the case of the vibrating-plate compactor, this effect appeared to increase the estimated compactor force above that measured by the direct instrumentation method.

- The pressure distribution beneath the base of the compactor can influence the embedded pressure cell readings. In the case of the rammer compactor operating on Light Castle sand, this effect appeared to increase the estimated compactor force above that measured by the direct instrumentation method.

- Use of a registration ratio of unity resulted in estimated compactor forces that were generally in as good, or better, agreement with the forces measured by the direct instrumentation as when in situ registration ratios were used.

During the in situ calibration studies, several factors that can influence the response of embedded pressure cells to static loads were identified:

- The presence of clods in the backfill can influence pressure cell response, even when the diaphragm size to soil particle size criterion is well satisfied. In general, pressure cells the size of the Kulite cells used in the study may be too small to yield consistent, reproducible results when used in field or model-scale studies.

- Compaction-induced lateral earth pressures can cause nonlinearity in pressure cell response because of the rotation of lateral stresses. This is similar to the nonlinearity seen in  $K_0$  unloading during laboratory calibration studies.

- In field or model-scale studies, other factors can influence pressure cell response, including (a) variations in cell placement conditions that are difficult to detect and (b) changes in cell placement condition during compaction of successive overlying lifts.

#### ACKNOWLEDGMENTS

This research was sponsored by the U.S. Army Corps of Engineers Waterways Experiment Station, Nikken Sekkei Ltd. of Japan, and Virginia Polytechnic Institute and State University. J. M. Duncan provided many useful suggestions during the course of the work. A. L. Sehn designed and constructed the instrumented retaining wall facility.

#### REFERENCES

1. Whiffen, A. C. The Pressures Generated in Soil by Compaction Equipment. *Symposium on Dynamic Testing of Soils*, Special Technical Publication 156. ASTM, Philadelphia, Pa., 1954, pp. 186–210.
2. Toombs, A. F. *The Performance of Bomag BW 75S and BW 200 Double Vibrating Rollers in the Compaction of Soil*. Transport and Road Research Laboratory Report LR 480. Transport and Road Research Laboratory, Crowthorne, England, 1972.
3. D'Appolonia, D. J., R. V. Whitman, and E. D'Appolonia. Sand Compaction with Vibratory Rollers. *Journal of the Soil Mechanics and Foundations Division*, ASCE, Vol. 95, No. 1, 1969, pp. 263–284.
4. Sehn, A. L., and J. M. Duncan. *Experimental Study of Earth Pressures on Retaining Structures*. Geotechnical Engineering Division, Department of Civil Engineering, Virginia Polytechnic Institute and State University, Blacksburg, 1990.
5. Filz, G. M., and J. M. Duncan. *An Experimental and Analytic Study of Earth Loads on Rigid Retaining Walls*. Geotechnical Engineering Division, Department of Civil Engineering, Virginia Polytechnic Institute and State University, Blacksburg, 1992.
6. Filz, G. M., and J. M. Duncan. Pressure Cell Drift. *Geotechnical Testing Journal*, ASTM, Vol. 16, No. 4, Dec. 1993, pp 432–441.
7. Filz, G. M., and T. L. Brandon. Instrumentation for Dynamic Compactor Force Measurements. *Geotechnical Testing Journal*, ASTM, Vol. 16, No. 4, Dec. 1993, pp 442–449.
8. Weller, W. A., Jr., and F. H. Kulhawy. Factors Affecting Stress Cell Measurements. *Journal of the Geotechnical Engineering Division*, ASCE, Vol. 108, No. 12, Dec. 1982, pp 1529–1548.
9. Kohl, K. M., B. M. New, and T. D. O'Rourke. Stress Cell Measurements for the Investigation of Soil-Pipeline Interactions During Vehicular Loading. *Instrumentation in Geotechnical Engineering*, TTL, London, 1989, pp 129–145.
10. Hadala, P. F. The Effects of Placement Method on the Response of Soil Stress Gages. *Proc., International Symposium on Wave Propagation and Dynamic Properties of Earth Materials*. The University of New Mexico Press, Albuquerque, pp 255–263.
11. Dunncliff, J. *Geotechnical Instrumentation for Monitoring and Field Performance*. John Wiley and Sons, Inc., New York.
12. Terzaghi, K., and R. Peck. *Soil Mechanics in Engineering Practice*. John Wiley and Sons, Inc., New York.